Medical Engineering and Physics 65 (2019) 61–67

Contents lists available at ScienceDirect

Medical Engineering and Physics

journal homepage: www.elsevier.com/locate/medengphy

Technical note

# Simplified parametric models of the dielectric properties of brain and muscle tissue during electrical stimulation

Peadar F. Grant[a,*], Madeleine M. Lowery[b]

[a] Department of Computing Science and Mathematics, School of Informatics and Creative Arts, Dundalk Institute of Technology, Dundalk, Co. Louth, Ireland
[b] UCD School of Electrical and Electronic Engineering, University College Dublin, Belfield, Dublin 4, Ireland

ARTICLE INFO

*Article history:*
Received 18 March 2017
Revised 26 March 2018
Accepted 16 December 2018

*Keywords:*
Electrical neural stimulation
Dispersion
Cole-Cole model
Debye model
Computational model

ABSTRACT

Parametric models are commonly used to describe the dispersive dielectric properties of biological tissues. While distinct regions of dispersion have been identified, the relative contribution of each during electrical stimulation is unknown. This study quantified the contribution of individual poles in parametric models of brain and muscle dielectric properties during electrical stimulation. The effect on the extracellular voltage waveform and threshold current for nerve stimulation of selectively removing subsets of poles from Cole-Cole and Debye models was examined. Errors were introduced when dispersions below 100 kHz were removed in both brain and muscle tissue. Poles below 1 kHz influenced the amplitude of the extracellular voltage waveform and the predicted minimum stimulation current. Poles between 1 kHz and 100 kHz influenced the waveform shape, with a minor effect on stimulus amplitude. The results confirm that low frequency dispersion in conductivity and permittivity can fundamentally influence the electric field and neural response during stimulation and provide insight into the relative contribution of the different dispersive regimes. Furthermore, they provide justification for for simplifying parametric models of dielectric properties through the removal of high frequency poles above 100 kHz which could improve the efficiency of time-domain solvers for simulations involving time-varying or aperiodic stimuli as may be required for certain closed-loop stimulation paradigms.



## 1. Introduction

Modeling the electric field induced during electrical stimulation is a vital component in understanding how electrical stimulation of nerves can modulate activity of the nervous system. Over the past several decades, it has provided insight into the various effects of electrode geometry, tissue electrical properties and neural response across a range of application areas. In the majority of modelling studies both to assess the efficacy of electrical stimulation and to simulate bioelectric signals, it is assumed that capacitive, inductive and propagation effects can be neglected [1], a simplification known as the quasi-static approximation [1–3]. Although inductive and propagation effects have been confirmed to be negligible for frequencies and volume conductor dimensions of interest [2], analytical and simulation studies have suggested that capacitive effects are the weakest of these three assumptions [2,4–6]. In the case of deep brain stimulation using chronically implanted electrodes, incorporation of tissue capacitance into models of the electric field has been shown to increase the minimum current required for axonal stimulation and reduce the estimated volume of excitable tissue activated by the stimulus [6–8].

Additionally, the electrical conductivities and permittivities of many biological tissues are known to vary as a function of excitation frequency [9–13]. Recent computational studies have shown that incorporating dielectric dispersion can influence the thresholds for neural stimulation and has the greatest effect under current controlled stimulation or voltage controlled stimulation when highly resistive encapsulation tissue surrounds the electrode [7,14], but has limited effect for voltage controlled stimulation when high-impedance encapsulation tissue is not present. Simulation studies have reported that frequency-independent resistive and capacitive approximations of the fully dispersive tissue model may provide accurate estimates of stimulation efficacy, subject to the properties' being estimated at an appropriate frequency [2,7].

Dielectric tissue models typically characterise dispersive tissue properties in the form of Debye, Lorenz or Cole-Cole models. These relations incorporate a series of dispersive poles that have been reported to correspond to different physical processes [11–13]. Dispersions at frequencies in excess of 1 GHz are attributed to polarisation of water molecules [11]. Similarly, poles within the range 1 MHz to 1 GHz correspond to polarisation of cellular membranes.

* Corresponding author.
*E-mail address:* peadar.grant@dkit.ie (P.F. Grant).

https://doi.org/10.1016/j.medengphy.2018.12.018
1350-4533/

**Table 1**
Stimulus parameters for brain tissue and muscle tissue.

| Parameter | | | Brain Tissue | Muscle Tissue |
|---|---|---|---|---|
| Repetition frequency | $f_p$ | | 100 Hz | 20 Hz |
| Pulse duration | $\tau_p$ | min | 50.0 μs | 100.0 μs |
| | | default | 400.0 μs | 400.0 μs |
| | | max | 400.0 μs | 1 μs |

Low frequency (below 1 MHz) dispersions correspond to ionic diffusion processes across the cell membrane [11]. Where simulation studies of the electric field have incorporated dispersive tissue properties, all dispersive poles for each biological tissue have been included [2,7]. As a result, the functional influence that individual dispersive poles and their corresponding physical processes exert on the efficacy of a given stimulus remains unknown.

Models which incorporated tissue capacitance, including those incorporating dispersion, have predominantly employed frequency-domain solution methods [2,6,7]. Incorporating a greater number of dispersive poles in frequency-domain solutions carries minimal additional memory storage requirements. However time-domain solutions require a linear increase in memory requirements corresponding to the addition of each dispersive poles [15]. Therefore, the ability to identify dispersive poles that do not functionally affect the predicted outcome of stimulation may be advantageous when attempting to simplify dispersive tissue models. Furthermore, analysis of the contribution of the different dispersive regions in the electrical conductivity and permittivity of biological tissues can provide insight into the physiological and physical processes that influence electrical stimulation of neural tissue. While it may intuitively be expected that the contribution of high frequency poles lying outside the frequency range of interest for stimulation will be negligible, it is possible that in the Debye, Lorenz or Cole-Cole formulation, neglect of individual poles may effect the distribution of conductivity and permittivity values at lower frequencies which may influence the distribution of the electric field during stimulation. Additionally, it is not known how low-frequency dielectric dispersions individually alter the electric field and subsequent thresholds for stimulation.

To address this, the aim of the present study was to quantify the effects of individual dispersive poles on the output waveform in the vicinity of the stimulating electrode and on the threshold for activation of a generalized mammalian axon in brain and muscle tissue.

## 2. Methods

Electrical stimuli were synthesised based on typical stimulation parameters for brain and muscle tissue. Using an analytical volume conductor model incorporating full dispersive tissue properties, the voltage waveform was determined at all nodes of a simulated mammalian axon model lying close to the electrode [16]. The effect of removing subsets of the available dispersive poles on the voltage waveform and minimum required stimulus amplitude for activation of the axonal fiber was then quantified.

### 2.1. Stimulus generation

Rectangular cathodic stimulus pulses were synthesised in the time-domain for a given pulse repetition frequency, $f_p$, and pulse duration, $\tau_p$, using 2000 terms of the trigonometric Fourier series. The Gibb's phenomenon was minimised by application of the Lanczos sigma approximation [17]. Stimulus parameters were chosen based on values typically used during deep brain stimulation [18] and neuromuscular electrical stimulation [19], Table 1. Samples were generated at frequency of $f_s$=1 MHz, which satisfied the Nyquist criterion for all tissues.

### 2.2. Tissue properties

The complex permittivity, $\hat{\varepsilon}$, of each biological tissue as a function of the angular frequency, $\omega$, was determined using the Cole-Cole equation

$$\hat{\varepsilon}(\omega) = \varepsilon_\infty + \sum_n \frac{\Delta\varepsilon_n}{1 + (\frac{j\omega}{f_n})^{(1-\alpha_n)}} + \frac{\sigma_i}{j\omega\varepsilon_0} \tag{1}$$

The behaviour of a given material is governed by the permittivity at infinity, $\varepsilon_\infty$, and the intrinsic conductivity, $\sigma_i$, at excitation frequencies of infinity and zero, respectively. Each individual dispersive pole, $n$, contributed an incremental complex relative permittivity, $\Delta\varepsilon_n$, at the pole frequency, $f_n$, which was spread by the parameter, $\alpha_n$. The Cole-Cole equation was applied to Debye materials by setting the $\alpha$ term to zero.

Brain tissue properties were estimated using the four-pole grey and white matter Cole-Cole models reported by Gabriel et al. [11], where each tissue model contained four dispersions, Table 2. Muscle tissue models were determined using the five-pole anisotropic model presented by Hurt [12].

### 2.3. Volume conductor model

An analytical homogeneous volume conductor of infinite extent was simulated, incorporating either isotropic brain tissue or anisotropic muscle tissue. Stimulation was delivered by a point source electrode [20], which injected a current $I_S$. The transfer function, $H$, which calculates the voltage at a distance $r$ from a unit input point current source within a medium having radial and longitudinal conductivities, $\hat{\sigma}_r$ and $\hat{\sigma}_z$, respectively, as a function of frequency was given by

$$H(r, z, \omega) = \frac{1}{4\pi\hat{\sigma}_r(\omega)\sqrt{r^2\frac{\hat{\sigma}_z(\omega)}{\hat{\sigma}_r(\omega)} + z^2}} \tag{2}$$

The periodic voltage waveform, $y$, in the tissue at a point at a distance $r$ from the stimulating electrode injecting current $x(t)$ was calculated using the Fourier transform, $\mathcal{F}$

$$y(r, z, t) = \mathcal{F}^{-1}[H(r, z, \omega) \cdot \mathcal{F}(x(t))] \tag{3}$$

Volume conductor simulations were implemented in Python using the SciPy FFT library [21].

### 2.4. Quantification of errors

For each biological tissue, dispersions were removed in order of highest to lowest frequency. As $n$ dispersive poles were removed, the voltage waveform, $y_n(t)$, at a given distance from the injected current was simulated. The error, $E_n$, compared to the voltage waveform, $y_0(t)$, incorporating all dispersions was calculated within the interval spanning the rising edge of the pulse at $t_0$ to the falling edge of the pulse at $t_0 + \tau_p$ as follows

$$E_n = \sqrt{\frac{1}{\tau_p}\int_{t=t_0}^{t=t_0+\tau_p}\left(\frac{y_n(t) - y_0(t)}{y_0(t)}\right)^2 \mathrm{d}t} \tag{4}$$

### 2.5. Calculation of neural activation thresholds

The effect of removing individual dispersive poles on the minimum stimulation amplitudes required to elicit action potential propagation was quantified using the myelinated mammalian axon model developed by McIntyre et al. [22]. Each axon included 21

**Table 2**
Parameters values used for Cole-Cole and Debye tissue models to calculate electrical properties. Each material is defined by $\varepsilon_\infty$, the relative permittivity at infinity, and $\sigma_i$, intrinsic conductivity. Each pole, $k$, contributes a change in relative permittivity, $\Delta\varepsilon_k$, at the pole frequency, $f_k$, spread by the parameter $\alpha_k$ in the case of Cole-Cole models. For Debye models, $\alpha_k$ is zero for all $k$. Brain tissue models have four poles, muscle tissue model has five poles [11,12].

| Material | Component | Ref | $\varepsilon_\infty$ | $\sigma_i$ | Pole | $k=1$ | $k=2$ | $k=3$ | $k=4$ | $k=5$ |
|---|---|---|---|---|---|---|---|---|---|---|
| Brain (grey matter) | Isotropic | [11] | 4.0 | 0.02 | $f_k$ | 30.0 Hz | 1.5 kHz | 10.0 MHz | 20.0 GHz | |
| | | | | | $\Delta\varepsilon_k$ | $4.50\times10^{7}$ | $2.00^{*}10^{5}$ | $4.00\times10^{2}$ | $4.50\times10^{1}$ | |
| | | | | | $\alpha_k$ | 0.0 | 0.22 | 0.15 | 0.1 | |
| Brain (white matter) | Isotropic | [11] | 4.0 | 0.02 | $f_k$ | 20.0 Hz | 3.0 kHz | 20.0 MHz | 20.0 GHz | |
| | | | | | $\Delta\varepsilon_k$ | $3.50\times10^{7}$ | $4.0\times10^{4}$ | $1.00\times10^{2}$ | $3.20\times10^{1}$ | |
| | | | | | $\alpha_k$ | 0.0 | 0.3 | 0.1 | 0.1 | |
| Muscle | Transverse | [12] | 4.3 | 0.0762 | $f_k$ | 69.0 Hz | 43.0 kHz | 670.0 kHz | 230.0 MHz | 20.0 GHz |
| | | | | | $\Delta\varepsilon_k$ | $2.00\times10^{5}$ | $8.19\times10^{4}$ | $1.19\times10^{4}$ | $3.20\times10^{1}$ | $4.58\times10^{1}$ |
| | | | | | $\alpha_k$ | 0.0 | 0.0 | 0.0 | 0.0 | 0.0 |
| Muscle | Parallel | [12] | 4.3 | 0.0446 | $f_k$ | 150.0 Hz | 38.0 kHz | 7.3 MHz | 370.0 MHz | 20.0 GHz |
| | | | | | $\Delta\varepsilon_k$ | $3.37\times10^{6}$ | $7.95\times10^{4}$ | $3.68\times10^{3}$ | $2.00\times10^{1}$ | $4.56\times10^{1}$ |
| | | | | | $\alpha_k$ | 0.0 | 0.0 | 0.0 | 0.0 | 0.0 |

nodes of ranvier, spaced at 500.0 μm intervals. The fiber diameter was set to 5.7 μm, and all diameter-dependent parameter values were set according to those reported in [22].

The multicompartment axon model was implemented in NEURON 7.3 in conjunction with the Python interpreter [23]. The voltage at each nodal and internodal compartment was calculated and applied as an extracellular potential. Numerical integration was performed using the Crank-Nicholson method using a time step of 1 μs. The Brent optimisation method, as implemented by the SciPy package [21], was used to determine the minimum stimulus current required to elicit action potential propagation in a myelinated axon located 5 mm from the stimulation point, to a tolerance of 1 pA.

Pulse durations were varied from 50.0 μs to 400.0 μs in the case of brain tissue, and from 100.0 μs to 1 μs in the case of muscle tissue. Simulations were conducted in parallel using the message-passing interface following the bulletin-board worker model [24]. Postprocessing was carried out using custom written Python 2.7 code.

### 2.6. Analysis of low-frequency poles

To examine the effects of the low-frequency poles, the $n$ highest-frequency poles for which the errors were less than 0.1 were removed. For the materials examined, the highest two poles were removed in brain tissue, $n=2$, and the highest three poles were removed in muscle tissue, $n=3$. The analysis was then repeated for the remaining subset of poles, with the first, $k=1$, and second, $k=2$, poles separately removed, so that their effects on the temporal voltage waveform and threshold stimulation amplitude could be isolated.

## 3. Results

### 3.1. Voltage waveforms in tissue

Temporal voltage waveforms for a portion of one stimulation period are presented in Fig. 1 for all tissues, for a representative stimulus pulse of 1 mA amplitude and duration 400 μs. Errors following the removal of $n$ poles ($n=1,2,5$) using Eq. (4) are detailed in Table 3.

For all tissues, errors were negligible when poles at frequencies in excess of 100 kHz were removed, $E_1$ and $E_2$ for brain and $E_1$, $E_2$ and $E_3$ for muscle in Table 3. In the case of grey matter, removal of the third pole in order of descending frequency caused an error of 6.06 which altered slightly the waveform shape Fig. 1(a). Removal of the final remaining pole resulted in an error of 44.31 and increased the peak magnitude of the voltage waveform by a factor of approximately four.

**Table 3**
Error, $E_n$, of the voltage waveform at a distance of 5 mm following the removal of $n$ poles in order of descending frequency. Values are presented for pulse durations of 400 μs.

| Material | $E_1$ | $E_2$ | $E_3$ | $E_4$ | $E_5$ |
|---|---|---|---|---|---|
| Brain (grey matter) | 0.00 | 0.01 | 6.06 | 44.31 | |
| Brain (white matter) | 0.00 | 0.00 | 3.16 | 11.84 | |
| Muscle | 0.00 | 0.00 | 0.05 | 0.67 | 46.65 |

**Table 4**
Stimulation current amplitude, $a_n$, in μA required to elicit axonal activation at a distance of 5 mm from the stimulus point current source. $n$ is the number of poles removed, in order of descending frequency.

| Material | $a_0$ | $a_1$ | $a_2$ | $a_3$ | $a_4$ | $a_5$ |
|---|---|---|---|---|---|---|
| Brain (grey matter) | 163 | 163 | 163 | 140 | 27 | |
| Brain (white matter) | 87 | 87 | 87 | 83 | 27 | |
| Muscle | 160 | 160 | 160 | 159 | 153 | 103 |

Similar results were observed for white matter, where removal of the third and fourth poles in order of descending frequency, resulted in errors of 3.16 and 11.84 relative to the case where all poles were included. A similar variation in shape to that observed in grey matter was observed, along with a slightly smaller increase in the peak amplitude of the waveform, Fig. 1(b).

In the case of muscle tissue, removal of the first two poles resulted in negligible errors, whilst the error following the removal of the third pole was 0.05, Table 3. Removal of the fourth pole resulted in a modification of the waveform shape, Fig. 1(c), and a corresponding error of 0.67. When the fifth pole was removed, the error increased to 46.65, however the increase in peak magnitude was less than that observed for brain tissues, Fig. 1.

### 3.2. Stimulation thresholds

Stimulation thresholds were determined for brain and muscle tissue, and are presented in Table 4. For brain tissues, the threshold current values for grey matter and white matter were unchanged as the two poles with the highest pole frequencies were removed from the parametric Cole-Cole model. Similarly, for muscle tissues, the required stimulation amplitude remained constant as the first three poles were removed in order of descending pole frequency, $k=\{5,4,3\}$.

In the case of grey matter, the required stimulation amplitude was reduced by 14.7% when the pole $k=2$ at 1.5 kHz was removed. When the pole $k=1$ at 30 Hz was additionally removed,

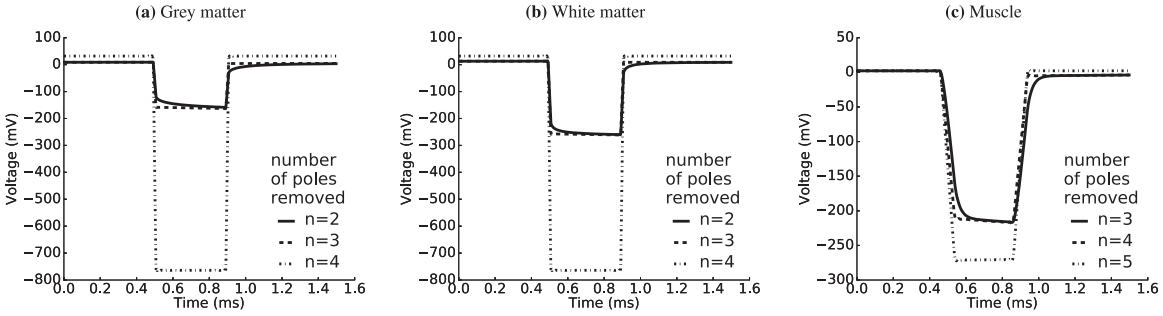


**Fig. 1.** Voltage waveforms 5 mm from the stimulating electrode in (a) grey matter, (b) white matter and (c) muscle due to stimulus of 1 mA amplitude and 400.0 μs duration. For each material, $n$ denotes the number of poles removed in order of descending frequency. For brain tissues, (a) and (b), as the error was negligible when the two highest poles were removed, the waveforms are omitted from the plots for reasons of clarity. In the case of muscle tissue, the cases of $n = 0, 1, 2$ poles removed are similarly omitted, (c).

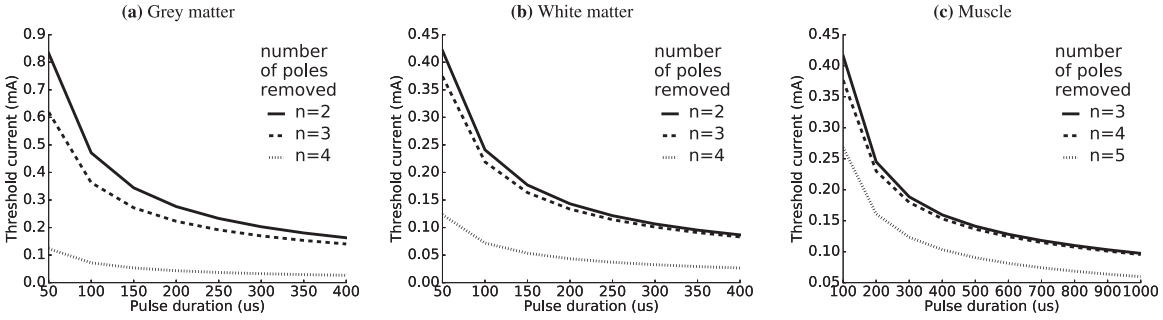


**Fig. 2.** Threshold current for stimulation, $a_n$, plotted with respect to stimulation pulse duration. $n$ is the number of poles removed, in order of descending frequency. For brain tissues, (a) and (b), as the error when one pole was removed, $k = 1$, was negligible, the waveforms are omitted from the plots for clarity. In the case of muscle tissue, (c), the cases of $n = 0, 1, 2$ poles removed are similarly omitted.

the stimulation amplitude was reduced by 85% relative to the case when all poles were included.

For white matter, removal of the pole $k = 2$ at 3.0 kHz resulted in a small reduction of 3.4% in the required stimulation amplitude to 83 μA. Removal of final remaining pole $k = 1$ at 20 Hz resulted in a reduction of 70.1% in the required stimulation amplitude relative to the case where all poles were included. In the case of muscle tissues, removal of the pole $k = 2$ at 38 kHz reduced the required stimulation amplitude by 3.9%, and removal of the final remaining pole at 150 Hz resulted in a reduction of 33.8% in the required stimulation amplitude relative to the case where all poles were included.

The minimum amplitudes for stimulation were then examined as pulse durations were varied, Fig. 2. The results remained consistent with the relative differences presented in Table 4 as pulse durations were varied from 50.0 μs to 400.0 μs for brain tissue, Fig. 2(a) and Fig. 2(b), and from 100.0 μs to 1 μs for muscle tissue, Fig. 2(c).

### 3.3. Individual effects of low-frequency poles

As removal of the poles at frequencies above 100 kHz resulted in negligible errors for all tissues, the effects of the two lowest-frequency poles were then individually examined, Fig. 3. All poles were removed and the effect of incorporating each of the two lowest frequency poles on the voltage waveform was estimated Fig. 4. Corresponding errors, with respect to the full dispersive solution, and threshold stimulus amplitudes when each of the low frequency poles were individually removed are presented in Table 5.

For grey and white matter brain tissues, removal of the lowest frequency pole, $k = 1$, increased the peak amplitude of the waveform, reducing the threshold stimulus amplitudes by 74.8% and 66.7% for grey and white matter respectively. A similar result was observed for muscle tissue, although the change in amplitude was of a smaller magnitude, Fig. 4(c). Similarly, the reduction in required stimulation amplitude of 31.8% was less than that for brain tissues. The relative effect of removing the two low-frequency poles remained consistent with the results presented in Table 5 as pulse durations were varied from 50.0 μs to 400.0 μs for brain tissue, Fig. 5(a) and Fig. 5(b), and from 100.0 μs to 1 μs for muscle tissue, Fig. 5(c).

## 4. Discussion

The aim of this study was to quantify the effect of using a subset of the available dispersive poles to describe the frequency-dependent electrical properties of brain and muscle tissue when estimating threshold amplitudes for neural stimulation. The results provide guidance on simplifying parametric models for dielectric tissues in computational studies of neural stimulation through the removal of high frequency poles. In addition, the specific effects of the remaining low-frequency poles were quantified.

As may be predicted from the frequency content of the simulus pulse, errors in the voltage waveform and stimulation thresholds were negligible when poles at frequencies in excess of 100 kHz were neglected, Table 3. The effects of the remaining two low-frequency poles, associated with diffusion processes at cell membranes [11], were examined separately. Removal of the lowest-frequency pole, situated within the frequency range 0 Hz to 1 kHz, caused an increase in the peak amplitude of the temporal voltage waveform, Fig. 4. This resulted in a consequential reduction in the minimum stimulus amplitude required to elicit neural activation, $a_1$, compared to that prior to removal, $a_0$, Table 5. A smaller, though still pronounced, effect was observed in muscle tissue compared to brain tissue. These observations indicate that poles at frequencies below 1 kHz primarily influence the magnitude of the voltage waveform, and therefore have a considerable effect on stimulus amplitudes required to elicit axonal activation.

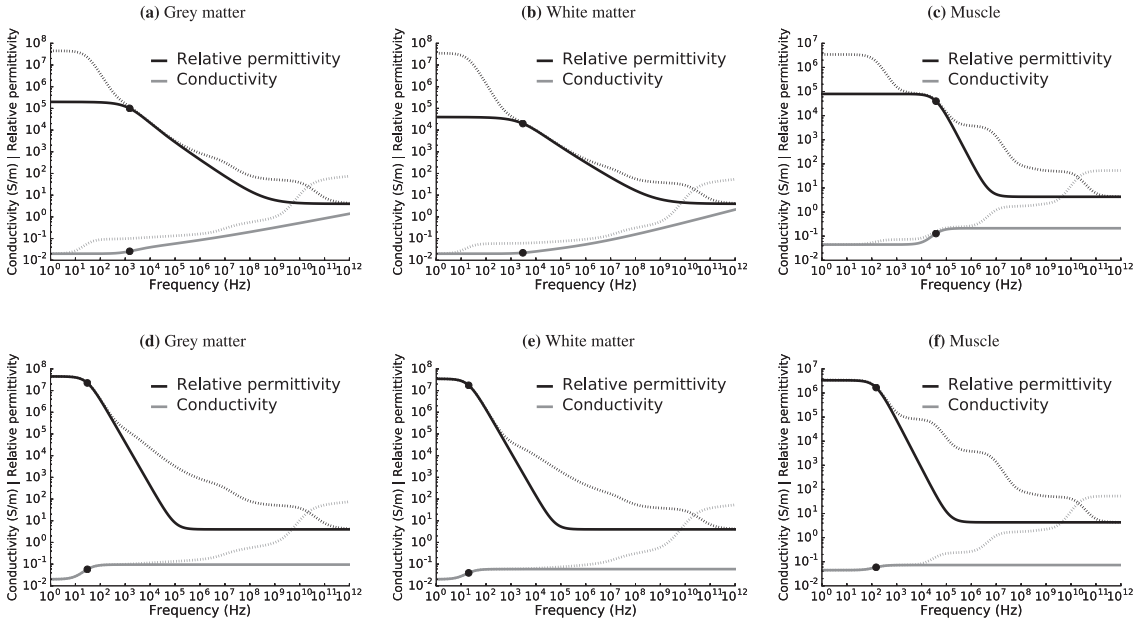


**Fig. 3.** Relative permittivity and electrical conductivity of (a,d) grey matter, (b,e) white matter and (c,f) muscle where the lowest, $k = 0$, pole was removed (a,b,c) and where the subsequent, $k = 1$, pole was removed (d,e,f). Dotted lines show comparison to the case where all poles are incorporated.

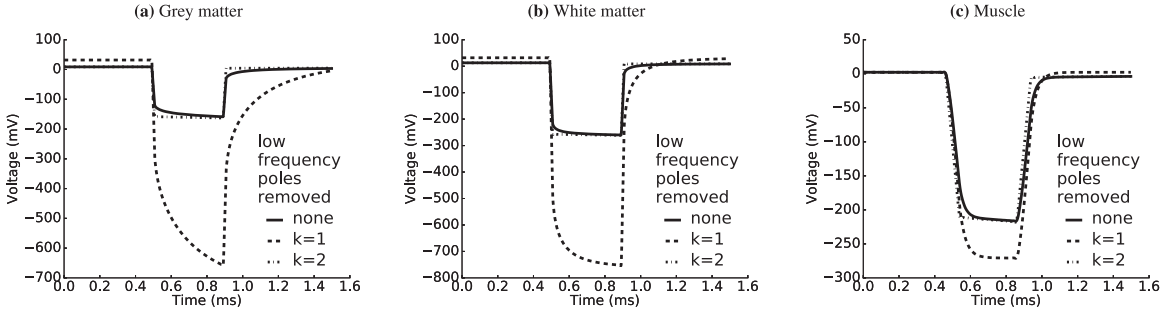


**Fig. 4.** Voltage waveforms in (a) grey matter, (b) white matter and (c) due to 1 mA stimulus. For brain tissues, (a) and (b), the highest two poles are removed. For muscle, (c), the highest three poles are removed. Figures show the voltage waveform when the lowest two poles, $k = \{1, 2\}$ are separately removed, compared to the case where no additional poles are removed.

**Table 5**
Error, $E_k$, of the voltage waveform and stimulation current amplitude, $a_k$, required to elicit axonal activation at a distance of 5 mm from the stimulus point current source for an axon located in a homogeneous medium following the removal of the $k$th lowest-frequency pole. For comparison, the $a_0$ case giving the threshold stimulus amplitude where no poles were removed is also presented.

| Material | $n$ highest-frequency poles removed | $a_{k=\emptyset}$ | Pole 1 removed | | Pole 2 removed | |
|---|---|---|---|---|---|---|
| | | | $E_{k=1}$ | $a_{k=1}$ | $E_{k=2}$ | $a_{k=2}$ |
| Brain (grey matter) | 2 | 163 μA | 118.63 | 40 μA | 7.81 | 140 μA |
| Brain (white matter) | 2 | 87 μA | 18.99 | 30 μA | 3.50 | 83 μA |
| Muscle | 3 | 159 μA | 84.70 | 107 μA | 1.11 | 153 μA |

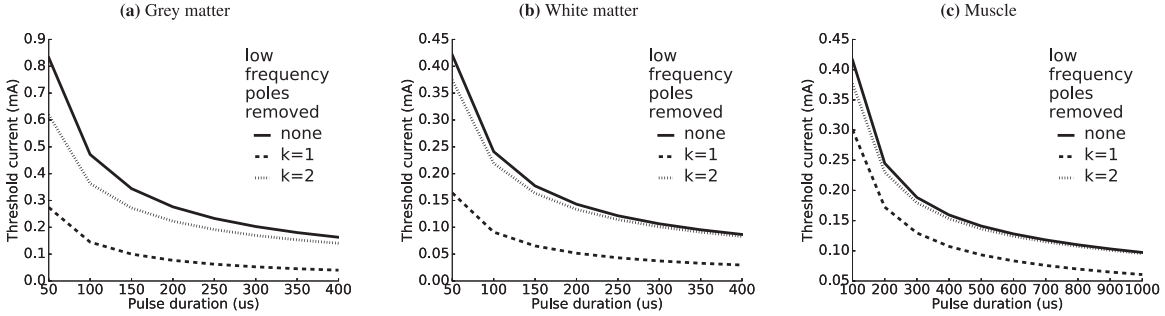


**Fig. 5.** Stimulation threshold, $a_n$, plotted with respect to stimulation pulse duration. $n$ is the number of poles removed, in order of descending frequency. For brain tissues, (a) and (b), as the error when no poles were removed and one pole was removed, $k = 1$, were both negligible, the waveforms are omitted from the plots for reasons of clarity. In the case of muscle tissue, the cases of $n = 0, 1, 2$ poles removed are similarly omitted, (c).

This can be seen also from the resulting distribution of the conductivity and relative permittivity, Fig. 3(a,b,c) where a substantial decrease in the tissue conductivity at frequencies greater than 10 Hz is observed when the lowest pole is removed, particularly in grey and white matter brain tissue.

The effect of removing poles within the range 100 kHz was then examined, and was found to primarily affect the shape of the waveform with a negligible change in its peak magnitude for all tissues, Fig. 4. This corresponded to small changes in the required stimulation amplitude necessary to elicit neural activation, $a_2$, compared to that required prior to the pole's removal, $a_0$, Table 5. This effect may be understood by considering the effect of removing the second pole on the conductivity and relative permittivity, Fig. 3(d,e,f) where the effect of removing the second pole is greatest on the relative permittivity at frequencies above approximately 100 Hz. The exact magnitude of the effect will depend on the precise neuron model used to determine the efficacy of the stimulus.

Although the results and conclusions drawn are likely to be of greatest interest to models utilising time-domain solvers, the analysis was conducted in the frequency domain to ensure computational uniformity across all simulations. The majority of published computational studies in the area of brain and muscle stimulation have employed similar frequency-domain approaches to that utilized in this work [2,6–8]. Dispersive media are easily simulated in this way, either in analytical point current-source models, or in finite element method applications that discretize the time-harmonic Laplace equation. Assuming a linear electrical tissue model, superposition permits dispersive frequency-dependent parametric tissue models to be utilised in place of fixed conductivities and permittivies. The frequency-domain approach imposes a number of limitations, and is most suited to periodic pulse waveforms where the stimulation parameters, other than amplitude, are fixed prior to simulation. However, several suggested stimulation paradigms involve the synthesis of arbitrary waveforms, the characteristics of which are not known a priori [25,26], and simulation of these approaches may be more suited to time-domain solution. Similarly, the simulation of closed-loop stimulation paradigms in which the frequency, waveform shape or duration of the stimulus pulse change as a function of time may be better approached using time-domain solvers. The results observed in this study have the potential to substantially reduce the memory storage requirements in time-domain simulations [15], which may improve the computational tractability of simulations involving time-varying or aperiodic stimuli.

This study was carried out subject to a number of limitations, which should be considered when interpreting the results and conclusions. The volume conductor was simulated using an analytical point current source model, as used in other field-neuron models [2,16]. This approach neglected the effects of several electromagnetic features such as the electrode-tissue interface [27], encapsulation tissue surrounding the stimulation electrode [28], tissue anisotropy [29], reference electrode [30] and more complex stimulation electrode geometries [7,31]. The overall findings of this study, however, should hold in the presence of more complex geometries though the exact values of the errors observed will vary according to the specifics of each model.

The sensitivity of the results to the parametric models of tissue impedance is complex and the results are specific to the parametric models chosen. The models of tissue dielectric properties by Gabriel et al. [11] used here are the most complete and extensively employed models of tissue dielectric properties currently available. The variation in conductivity and permittivity with frequency follows a well-defined curve, that is understood also in term of the underlying tissue composition. The overall shape of the dielectric curves is thus unlikely to vary across different measurement conditions and experiments. Nevertheless, the measurement of tissue dielectric properties at the relatively low frequencies of interest here is challenging and there is considerable variation in the values that have been reported for the same tissue in different species and under different experimental conditions.

The analysis has been confined to the frequency range where inductive and propagation effects are negligible, which is the case for the frequencies of interest during electrical neural stimulation [1,2]. The parametric models used to characterize the electrical properties of the biological tissues are based on experimental studies and individual parameters are subject to uncertainties [32], which have been shown to be capable of altering the resulting shape and extent of the region of neural tissue activated [33]. Cole-Cole parametric models were available for brain tissues [11], however, only Debye parameterizations were available for muscle tissues [12]. Measurements *in-vivo* exhibit a slightly greater frequency response in the conductivity and differences in the magnitude and frequency response of the relative permittivity, related to the different responses of lower and higher frequency dispersions following cell death [34].

## 5. Conclusion

The effect of individual poles in the dielectric dispersion of brain and muscle tissue on the volume conducted voltage waveform and thresholds for nerve electrical stimulation were examined using model simulation. Removal of poles below 100 kHz resulted in errors in the voltage waveform and, consequentially, in the minimum stimulus amplitudes necessary to elicit axonal activation. For all tissues, poles at frequencies between zero and 1 kHz primarily influenced the voltage waveform's magnitude, and had the greatest effect on predicted minimum stimulation amplitudes. Poles at frequencies from 100 kHz influenced the voltage waveforms shape, and had a relatively minor effect on required minimum stimulus amplitudes. The results support the simplification of classic models of dielectric dispersion under these conditions. These simplifications would be of particular benefit in the design of time-domain numerical solvers for simulating time-varying stimulation as may occur, for example, in closed-loop stimulation paradigms.

## Acknowledgments

1. This work is supported in part by ERC Consolidator Grant ERC-2014-CoG 646923 DBSModel. 2. The authors acknowledge the Research IT Service at University College Dublin (http://www.ucd.ie/itservices/researchit/) and the Irish Centre for High-End Computing for providing HPC resources that have contributed to the research results reported within this paper.

## References

[1] Plonsey R, Heppner DB. Considerations of quasi-stationarity in electrophysiological systems. Bull Math Biophys 1967;29(4):657–64.
[2] Bossetti CA, Birdno MJ, Grill WM. Analysis of the quasi-static approximation for calculating potentials generated by neural stimulation. J Neural Eng 2008;5(1):44–53.
[3] Mesin L, Merletti R. Distribution of electrical stimulation current in a planar multilayer anisotropic tissue. IEEE Trans Biomed Eng 2008;55(2 Pt 1):660–70.
[4] Stoykov NS, Lowery MM, Taflove A, Kuiken TA. Frequency- and time-domain fem models of EMG: capacitive effects and aspects of dispersion. IEEE Trans Biomed Eng 2002;49(8):763–72.
[5] Lowery MM, Stoykov NS, Dewald JPA, Kuiken TA. Volume conduction in an anatomically based surface EMG model. IEEE Trans Biomed Eng 2004;51(12):2138–47.
[6] Butson CR, McIntyre CC. Tissue and electrode capacitance reduce neural activation volumes during deep brain stimulation. Clin Neurophysiol 2005;116(10):2490–500.
[7] Grant PF, Lowery MM. Effect of dispersive conductivity and permittivity in volume conductor models of deep brain stimulation. IEEE Trans Biomed Eng 2010;57(10):2386–93. doi:10.1109/TBME.2010.2055054.

[8] Yousif N, Liu X. Investigating the depth electrode-brain interface in deep brain stimulation using finite element models with graded complexity in structure and solution. J Neurosci Methods, DOI: http://dx.doi.org/10.1016/j.jneumeth.2009.07.005.
[9] Gabriel C, Gabriel S, Corthout E. The dielectric properties of biological tissues: I. literature survey. Phys Med Biol 1996;41(11):2231–49.
[10] Gabriel S, Lau RW, Gabriel C. The dielectric properties of biological tissues: II. measurements in the frequency range 10 Hz to 20 GHz. Phys Med Biol 1996;41(11):2251–69.
[11] Gabriel S, Lau RW, Gabriel C. The dielectric properties of biological tissues: III. parametric models for the dielectric spectrum of tissues. Phys Med Biol 1996;41(11):2271–93.
[12] Hurt WD. Multiterm Debye dispersion relations for permittivity of muscle. IEEE Trans Biomed Eng 1985;32(1):60–4.
[13] Logothetis NK, Kayser C, Oeltermann A. In vivo measurement of cortical impedance spectrum in monkeys: implications for signal propagation. Neuron 2007;55(5):809–23.
[14] Tracey B, Williams M. Computationally efficient bioelectric field modeling and effects of frequency-dependent tissue capacitance. J Neural Eng 2011;8(3):036017.
[15] Stoykov NS, Kuiken TA, Lowery MM, Taflove A. Finite-element time-domain algorithms for modeling linear Debye and lorentz dielectric dispersions at low frequencies. IEEE Trans Biomed Eng 2003;50(9):1100–7.
[16] Grant PF, Lowery MM. Contribution of dielectric dispersions to voltage waveforms arising from electrical stimulation. In: Proceedings of the 34th international IEEE engineering in medicine and biology conference; 2012. p. 4148–51. doi:10.1109/EMBC.2012.6346880.
[17] Jerri AJ. The Gibbs phenomenon in fourier analysis. In: Splines and Wavelet Approximations. Kluwer Academic Publishers; 1998.
[18] Volkmann J, Herzog J, Kopper F, Deuschl G. Introduction to the programming of deep brain stimulators. Mov Disord 17 Suppl 2002;3. S181–7
[19] Doucet BM, Lam A, Griffin L. Neuromuscular electrical stimulation for skeletal muscle function. Yale J Biol Med 2012;85(2):201–15.
[20] McIntyre CC, Grill WM. Finite element analysis of the current-density and electric field generated by metal microelectrodes. Ann Biomed Eng 2001;29(3):227–35.
[21] Jones E, Oliphant T, Peterson P, et al. SciPy: Open source scientific tools for Python. 2001.
[22] McIntyre CC, Richardson AG, Grill WM. Modeling the excitability of mammalian nerve fibers: influence of afterpotentials on the recovery cycle. J Neurophysiol 2002;87(2):995–1006.
[23] Hines ML, Carnevale NT. The NEURON simulation environment. Neural Comput 1997;9(6):1179–209.
[24] Hines ML, Carnevale NT. Translating network models to parallel hardware in NEURON. J Neurosci Methods 2008;169(2):425–55.
[25] Popovych O, Hauptmann C, Tass P. Demand-controlled desynchronization of brain rhythms by means of nonlinear delayed feedback. Conf Proc IEEE Eng Med Biol Soc 2005;7:7656–9.
[26] Hauptmann C, Tass PA. Therapeutic rewiring by means of desynchronizing brain stimulation. Biosystems 2007;89(1-3):173–81.
[27] Cantrell DR, Inayat S, Taflove A, Ruoff RS, Troy JB. Incorporation of the electrode-electrolyte interface into finite-element models of metal microelectrodes. J Neural Eng 2008;5(1):54–67.
[28] Grill WM, Mortimer JT. Electrical properties of implant encapsulation tissue. Ann Biomed Eng 1994;22(1):23–33.
[29] McIntyre CC, Mori S, Sherman DL, Thakor NV, Vitek JL. Electric field and stimulating influence generated by deep brain stimulation of the subthalamic nucleus. Clin Neurophysiol 2004;115(3):589–95.
[30] Grant PF, Lowery MM. Electric field distribution in a finite-volume head model of deep brain stimulation. Med Eng Phys 2009;31(9):1095–103. doi:10.1016/j.medengphy.2009.07.006.
[31] Butson C, McIntyre C. Current steering to control the volume of tissue activated during deep brain stimulation. Brain Stimulat 2008;1(1):7–15.
[32] Gabriel C, Peyman A, Grant EH. Electrical conductivity of tissue at frequencies below 1 MHz. Phys Med Biol 2009;54(16):4863–78. doi:10.1088/0031-9155/54/16/002.
[33] Schmidt C, Grant P, Lowery M, van Rienen U. Influence of uncertainties in the material properties of brain tissue on the probabilistic volume of tissue activated. IEEE Trans Biomed Eng 2013;60(5):1378–87. doi:10.1109/TBME.2012.2235835.
[34] Wagner T, Eden U, Rushmore J, Russo CJ, Dipietro L, Fregni F, Simon S, Rotman S, Pitskel NB, Ramos-Estebanez C, Pascual-Leone A, Grodzinsky AJ, Zahn M, Valero-Cabré A. Impact of brain tissue filtering on neurostimulation fields: a modeling study. Neuroimage 85 Pt 2014;3:1048–57. doi:10.1016/j.neuroimage.2013.06.079.